Strip Waveguide Enabling Low Loss for Silicon on Silica Technology in the MIR

Mina Labib
Engineering Physics and Mathematics Department,
Faculty of Engineering, Ain Shams University,
Cairo, Egypt.
mina.sobhy.labib@eng.asu.edu.eg

Michael Gad
Engineering Physics and Mathematics Department,
Faculty of Engineering, Ain Shams University,
Cairo, Egypt.
mmonirmo@eng.asu.edu.eg

Yasser M Sabry
Electronics and Communication Engineering Department,
Faculty of Engineering, Ain Shams University,
Cairo, Egypt.
yasser.sabry@eng.asu.edu.eg

Diaa Khalil
Electronics and Communication Engineering Department,
Faculty of Engineering, Ain Shams University,
Cairo, Egypt.
Diaa.khalil@ieee.org

***Abstract*—Mid-infrared silicon photonics is attracting academic and industrial interest due to the potential applications in chip-scale sensors, free-space optical communications in addition to others. This work offers a technique to push the limit of silicon photonics using the traditional silicon on silica technology deeper into the mid-infrared region, up to a wavelength of 4.28 μm, despite the extensive silica absorption losses. It is demonstrated that a waveguide of 400 nm height and 1600 nm width requires a buried oxide buffer of 3.5 μm so that the leakage loss is below 0.01 dB/cm. The silica absorption loss in this case is only 3.4 dB/cm. In this approach, the silicon on silica platform can be employed for photonic devices, such as gas sensors, in that range of wavelength.**

Keywords—integrated optics; silicon photonics; mid-infrared; sensors; waveguides; photonic devices.

I. INTRODUCTION

The main driving force for using silicon on silica as a technology platform for photonics has always been utilizing the well-established complementary oxide semiconductor (CMOS) industry in producing photonic devices to work on-chip along with electronic devices [1]. Extensive work has been invested in order to provide the market with optimal devices that combine the best features of electronics and photonics. High speed and long-haul data transfer are the most attractive features of photonics, while miniature size and on-chip low-power consumption are the most attractive on the electronics side [2-3].

So far silicon-on-silica based photonics has been very successful in the implementation of key photonic devices in the near-infrared (NIR) range [4-5] such as directional couplers, Y-junctions, Mach-Zehnder interferometers, Bragg gratings, multi-mode interferometers, phased array waveguides, ring resonators [6] and electro-optic modulators [7]. Those devices were extensively used to design a wide range of photonic circuits such as filters [8], interleavers [9-10], sensors [11] and gyroscopes [12].

Nevertheless, silicon-on-silica platform brings new challenges to photonics circuit design. One of the main challenges is that silicon is an indirect band-gap material that does not generate laser. This is a topic that grabbed a lot of attention over the past decade, with some successful solutions, including fiber-grating couplers that provide silicon chips with laser from an external source [13]. More recently, there is a new trend of designing devices for mid-infrared (MIR) applications [14], for which the material absorption loss of silica beyond the wavelength of 3.8 μm is another challenge that comes into play.

This absorption has limited the use of the silicon-on-silica platform in vital applications such as gas sensing, knowing that gases have their strong absorption lines mainly in the mid infrared regime [15]. This is away from the commonly used telecommunication wavelengths of 1.31 μm and 1.55 μm in the NIR, where silicon and silica are transparent. The proposed solutions to this cumbersome issue navigated toward using alternative materials to silica such as silicon nitride, and sapphire [16, 17]. Such materials possess very small absorption at such MIR wavelengths and yet provide a large refractive index contrast with silicon, which enables small size devices; i.e. high density of integration. Besides sensing at the MIR wavelengths, other attractions present themselves such as higher fabrication tolerance [14], lower side-wall scattering losses [14], [18] and stronger free-plasma effect, which is useful for electro-optic modulation [14].

In this work, a solution to circumvent the silica absorption issue is proposed. The idea is based on changing the dimensions of the waveguide in order to decrease the overlap between the propagating mode profile and the buried silica underneath the silicon core. The waveguide structure and materials are presented in section II. The numerical simulation results are given in section III. Finally, the work is concluded in section IV.

II. MATERIAL PROPERTIES

In this study, the waveguide is strip type with a rectangular cross section of height H and width W. The core is made of silicon that lies on top of silica. The two sides of the waveguide core and its top are exposed to air, as shown in Fig. 1. The wavelength of operation is chosen to be 4.28 µm. At this wavelength, carbon dioxide (CO_2) possesses a significant optical absorption [14], [16]. Therefore, in this study the way is paved for a futuristic CO_2 silicon-on-silica integrated sensor. The optical properties of silicon and silica [16] at this wavelength are listed in Table 1. The numerical simulations are carried out using MODE from Lumerical, which is a finite difference eignemode solver [19].

TABLE 1: Optical properties of silicon and silica at λ_o=4.28 µm [16].

Material	Refractive index	Absorption loss (dB/cm)
Si	3.43	0.008
Silica	1.38	20

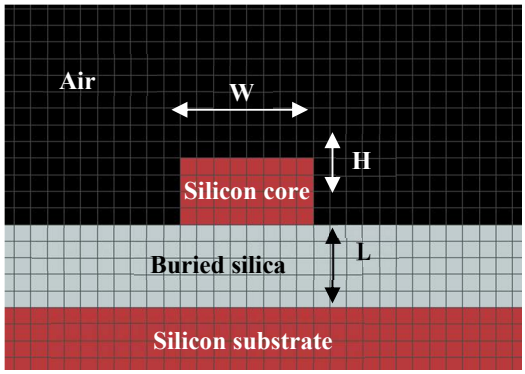

Fig. 1. The waveguide materials and dimensions.

III. RESULTS

A. Modal analysis

First, the waveguide height is chosen larger than the traditional 220 nm in order to confine the optical power more inside the transparent silicon core. In this study we investigate H = 400 nm. The function of the buried oxide thickness, L, is to block power leakage to the silicon substrate. In order to, temporarily, eliminate the effect of the leakage loss from our study, the buried oxide thickness is taken as L=15 µm which resembles a semi-infinite oxide layer as will be shown later in this work. This means that the calculated propagation loss at this stage is due to only silica absorption. Using the eignemode solver, the waveguide modes are found for different waveguide widths. The variation of the real effective index, n_e, the imaginary effective index, k, and the power absorption loss, $\alpha=4.343\times4\pi k/\lambda_o$ (dB/cm), versus the waveguide width in the range $0<W<3.3$ µm, is shown in Fig. 2, Fig. 3 and Fig. 4, respectively.

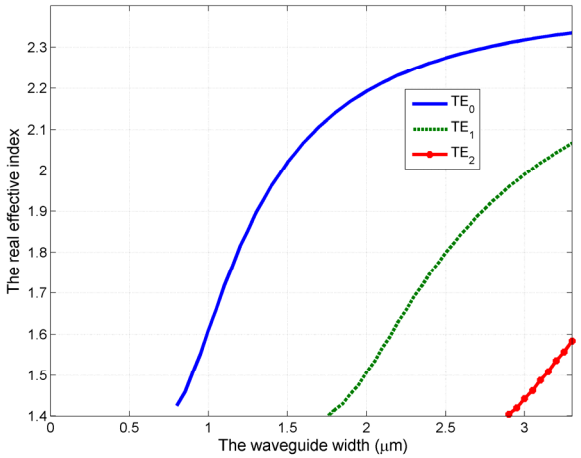

Fig. 2. The real effective index, for the first three modes, versus the waveguide width. The waveguide height is H=400 nm, the buried oxide thickness is L=15 µm and the free space wavelength is λ_o=4.28 µm.

For such waveguides, usually the modes are sorted in two groups, TE-like modes, with the main electric field component parallel to the substrate, and TM-like modes, with the main electric field component normal to the substrate Noticeably, while the fundamental TE-like mode, TE_0, has a cut off waveguide width of 800 nm, this waveguide does not support TM-like mode in the range of width in this study. Obviously, the TM-like mode is more affected by H than W and with such relatively small height the TM-mode does not show. Also, as expected, a higher order mode is less confined inside the core and hence experiences a larger absorption loss.

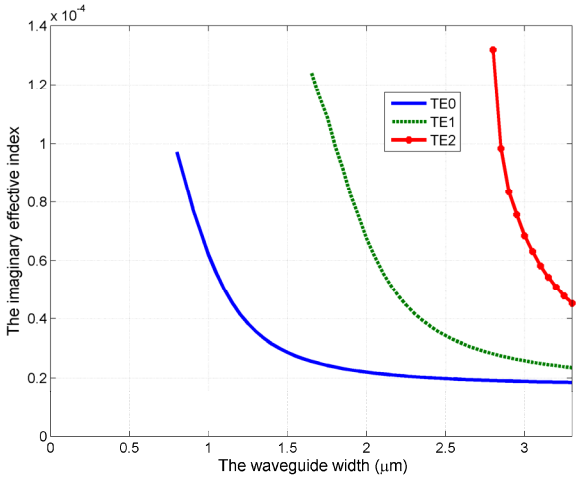

Fig. 3. The imaginary effective index, for the first three modes, versus the waveguide width. The waveguide height is H=400 nm, the buried oxide thickness is L=15 µm and the free space wavelength λ_o=4.28 µm.

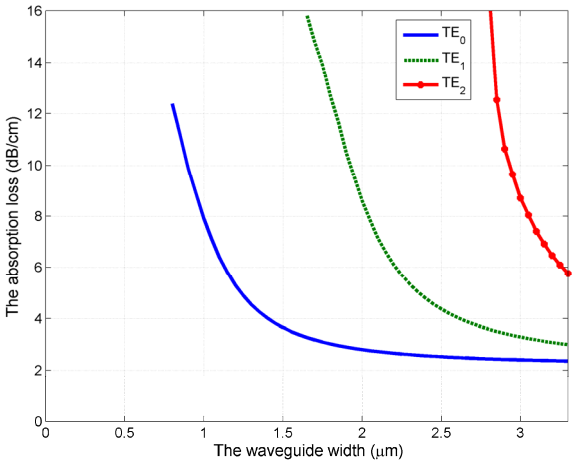

Fig. 4. The absorption loss, for the first three modes, versus the waveguide width. The waveguide height is H=400 nm, the buried oxide thickness is L=15 μm and the free space wavelength is λ_o=4.28 μm.

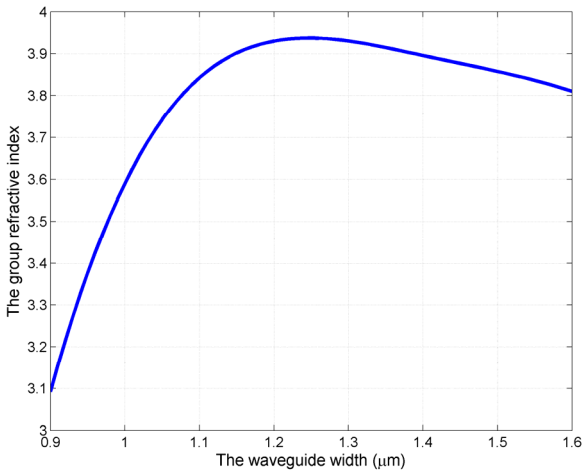

Fig. 5. The group refractive index for the fundamental mode versus the waveguide width. The waveguide height is H=400 nm, the buried oxide thickness is L=15 μm and the free space wavelength is λo=4.28 μm.

Since a single mode waveguide is more favorable in many applications, we will next focus on the fundamental mode for this waveguide. This waveguide supports a single mode as long as its width lies between 850 nm and 1700 nm. The group refractive index, $n_g = n_e - \lambda_o \, dn_e/d\lambda_o$, is plotted versus the waveguide width in Fig. 5. The group index has a peak value of about 3.93 for a waveguide width of about 1.25 μm.

B. Evanescent field ratio

The evanescent field ratio (EFR) is defined as the ratio of the mode power in the cladding, here air, to the total mode power [17]. This value is very important for the design of a sensor, since it determines how much of the mode power interacts with the sensor target material. As the EFR increases, the sensitivity of the waveguide increases. The change of the fundamental mode EFR with the waveguide width is depicted in Fig. 6. Again, as the waveguide width increases, more power is confined inside the core, which means lower EFR. A wider waveguide has a smaller EFR but also a smaller absorption loss, and as will be shown shortly, a smaller leakage loss. So, the waveguide width becomes a matter of a trade-off between the loss and the sensitivity.

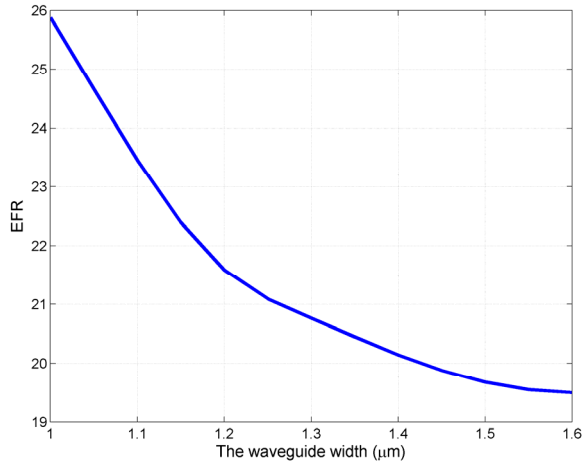

Fig. 6. The evanescent field ratio for the fundamental mode versus the waveguide width. The waveguide height is H=400 nm, the buried oxide thickness is L=15 μm and the free space wavelength is λ_o=4.28 μm.

C. Leakage loss

The last step is to find the proper values for L to stop power leakage to the substrate. Here, the mode solver is used to find the total power loss in (dB/cm) as a function of L for different widths. The results are limited to the fundamental mode and are illustrated in Fig. 7. This loss, unlike with L=15 µm, includes not only the silica absorption loss but also the leakage loss. Obviously, as L increases, the total loss decreases. Eventually, L reaches a value, call it L_a, where the leakage becomes negligible and the total loss saturates at a value that corresponds to silica absorption only. Also, as can be easily anticipated, as the waveguide width increases, more mode power is confined inside the waveguide transparent silicon core and hence the mode experiences lower absorption and lower leakage loss. This means that L_a is smaller for a wider waveguide. In Table 2, the value of L_a is given for different waveguide widths along with the corresponding absorption loss. The criterion we used to choose the value of L_a in this table is that the corresponding leakage loss is smaller than 0.01 dB/cm. From Fig. 7, subtracting the absorption loss value at $L=L_a$ from the total loss that corresponds to $L< L_a$, the absorption loss can calculated, and then plotted as in Fig. 8. The remarkable outcome of this work is that, as shown in Table 2, a waveguide of H=400 nm, W=1600 nm and buried oxide of L=3.5 µm can serve for integrated silicon-on-silica devices at λ_o=4.28 µm with a silica absorption loss penalty of only approximately 3.4 dB/cm and negligible leakage. Since the waveguide scattering loss is smaller at larger wavelengths, hence saving on the total loss budget is expected.

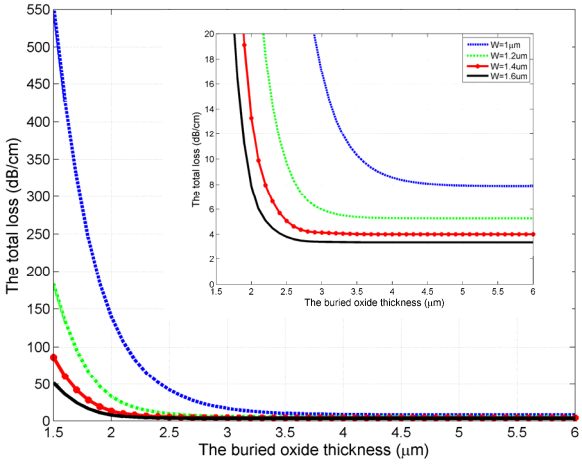

Fig. 7. The total loss, for the fundamental mode, versus the buried oxide thickness for different widths. The waveguide height is H=400 nm, and the free space wavelength is λ_o=4.28 µm. The inset shows a zoom in on the range of the total loss below 20 dB/cm.

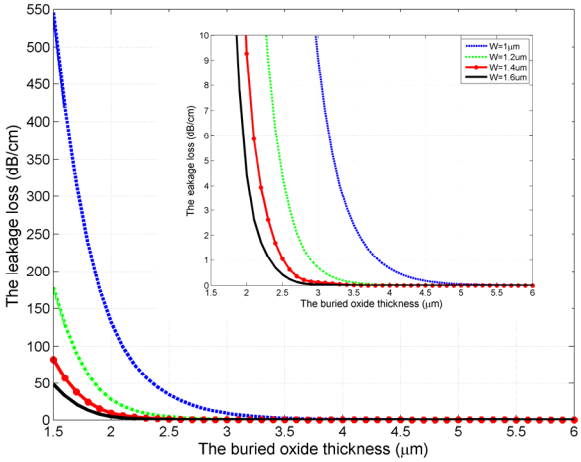

Fig. 8. The leakage loss, for the fundamental mode, versus the buried oxide thickness for different widths. The waveguide height is H=400nm, and the free space wavelength is λ_o=4.28µm. The inset shows a zoom in on the range of the leakage loss below 10 dB/cm.

TABLE 2: The buried oxide thickness for leakage loss smaller than 0.01 dB/cm for different waveguide widths and the corresponding the silica absorption loss. The waveguide height is H=400 nm and the operating wavelength is λ_o=4.28µm

W (µm)	L_a(µm)	Absorption loss (dB/cm)
1	6	7.9
1.2	4.5	5.3
1.4	4	4
1.6	3.5	3.4

At the wavelength of 1.55 µm, typical scattering losses of a silicon on silica strip waveguide range around 2 dB/cm [20]. At higher wavelengths, the losses vary according to the used materials besides the dimensions and the wavelength. A comparison between different technologies is shown in Table 3.

TABLE 3: Propagation losses for different technologies.

Reference	Technology	Wavelength (µm)	Losses (dB/cm)
[17]	Si on sapphire	4.23	2-5[a]
[18]	Si on silica	2.02	3.3[b]
[21]	Si on silica	3.8	3-6[b]
[22]	Si on nitride	3.39	5.2[c]
[23]	Suspended silicon waveguide	3.8	3.4[b]

a. Theoretical work.

b. Experimental work.

c. Experimental work for a ridge (not strip) waveguide.

The proposed waveguide structure in this work shows an absorption loss of 3.4 dB/cm at 4.28 µm. It is plausible to assume the same scattering losses of the closest wavelength in the previous table which is 2-5 dB/cm for silicon on sapphire waveguides [17]. Therefore, that the additional absorption loss

is in the same range as of the expected scattering losses. This means that the penalty for preserving the vital CMOS technology, beyond the limit of lossless silica, is acceptable and therefore the proposed waveguide represents a first step toward a CO_2 integrated sensor.

IV. CONCLUSION

A 400 nm high silicon on silica waveguide was optimized for lowest leakage and absorption losses at an operating wavelength of 4.28 µm. If the buried silica layer is 3.5 µm thick, the expected leakage loss is below 0.01 dB/cm and the silica absorption is limited to 3.4 dB/cm. This outcome makes this waveguide a potential building element for a CO_2 integrated sensor while preserving the mature silicon-on-silica technology.

V. REFERENCES

[1] Y. Chen et al, "A 25 Gb/s hybrid integrated silicon photonic transceiver in 28 nm CMOS and SOI," ISSCC 2015, DOI: 10.1109/ISSCC.2015.7063096.

[2] E. Agrill et al, "Roadmap of optical communications," Journal of Optics, vol. 18, no. 063002, 2016.

[3] D. Thomson et al, "Roadmap on silicon photonics," Journal of Optics, vol. 18, no. 073003, 2016.

[4] H. Subbaraman et al, "Recenet advances in silicon-based passive and active optical interconnects," Optics Express, vol. 23, pp. 2487-2510, 2015.

[5] D. Dai, "Silicon Nanophotonic Integrated Devices for On-chip Multiplexing and Switching." Journal of Lightwave Technology, vol. 35, pp. 572-587, 2017.

[6] M. Gad, D. Yevick and P. E. Jessop, "A comparison of modeling methods for ring resonator circuits," Journal of Optical Society of America A, vol. 27, pp. 703-708, 2010.

[7] M. Gad, D. Yevick and P. E. Jessop, "Tunable polymer/silcion over insulator ring resonators," Optical Engineering, vol. 47, no. 12, 2007.

[8] B. Jalali and S. Fathpour, "Silicon photonics," Journal of Lightwave Technology, vol. 24, pp. 4600-4615, 2006.

[9] M. Gad, D. Yevick and P. E. Jessop, "Compound ring resonator circuit for integrated optics applications," Journal of Optical Society of America A, vol. 26, pp. 2023-2032, 2009.

[10] M. Gad, J. Ackert, D. Yevick, L. Chrostowski and P. E. Jessop, "Ring resonator wavelength division multiplexing interleaver," Journal of Lightwave Technology, vol. 29, pp. 2102-2108, 12, 2011.

[11] V. Passaro, F. Dell'Olio, B. Casamassima and F. De Leonardis,"Guided-wave optical biosensors," Sensors, vol. 7, pp. 508-536, 2007.

[12] M. Gad, D. Yevick and P. E. Jessop, "High Sensitivity ring resonator gyroscopes," Fiber and Integrated Optics, vol. 30, pp. 395-411, 2011.

[13] M. Gad, A. Zaki and Y. M. Sabry, "Silicon photonic mid-infrared grating coupler based on silicon-on-insulator technology," NRSC 2017, pp. 400-406.

[14] R. Soref, "Mid-infrared photonics in silicon and germanium," Nature Photonics, vol. 4, pp. 495-497, 2010.

[15] J. Hodgkinson and R. P. Tatam, "Optical gas sensing: a review," Measurement Science and Technology, vol. 24, pp. no. 012004, 2013.

[16] S. J. Emelett and W. Buchwald, Silicon waveguided components for the long-wave infrared region," Journal of optics A: Pure and Applied Optics, vol. 8, pp. 840-848, 2006.

[17] Y. Huang, S. K. Kalyoncu, Q. Zhao, R. Torun and O. Boyraz, "Silicon-on-sapphire waveguides design for mid-IR evanescent field absorption gas sensors," Optics Communications, vol. 313, pp. 186-194, 2013.

[18] D. E. Hagan and A. P. Knights, "Mechanisms for optical loss in SOI waveguides for mid-infrared wavelengths around 2 µm," Journal of Optics, vol. 19, no. 025801, 2017.

[19] www.Lumerical.com

[20] W. Bogaerts et al, "Silicon microring resonators," Laser Photonics Review, vol. 6, pp. 47-73, 2011.

[21] M. muneeb et al, ",Demonstration of Silicon-on-insulator midinfrared spectrometers operating at 3.8µm," Optics Express, vol. 21, pp. 11659-11669, 2013.

[22] S. khan, J. Chiles, J. Ma and S. Fathpour, "Silicon-on-nitride waveguides for mid- and near-infrared integrated photonics," Applied Physics Letters, vol. 102, no. 121104, 2013.

[23] J. S. Penades et al, "Suspended SOI waveguide with sub-wavelength grating cladding for mid-infrared," Optics Letters, vol. 19, pp. 5661-5664, 2014.